12 (2022) 100277

Contents lists available at ScienceDirect

Biosensors and Bioelectronics: X

journal homepage: www.journals.elsevier.com/biosensors-and-bioelectronics-x

Naked-eye detection of antibiotic resistance gene *sul1* based on aggregation of magnetic nanoparticles and DNA amplification products

Darío Sánchez Martín [a], Marie Wrande [b], Linus Sandegren [b], Teresa Zardán Gómez de la Torre [a,*]

[a] Department of Material Sciences and Engineering, Division of Nanotechnology and Functional Materials, Uppsala University, Ångström Laboratory, 75121, Uppsala, Sweden
[b] Department of Medical Biochemistry and Microbiology, Uppsala University, Uppsala Biomedical Centre, 75123, Uppsala, Sweden

ARTICLE INFO

Keywords:
Antibiotic resistance
Point of care diagnostics
DNA detection
Magnetic nanoparticles
DNA aggregation

ABSTRACT

The continued spread of antimicrobial resistance is a global problem. In fact, the WHO has declared antimicrobial resistance one of the top 10 global public health threats facing humanity. Molecular methods offer a faster means of characterizing resistant strains than phenotypic drug susceptibility testing. We have developed a molecular detection method that generates visible aggregates from DNA amplified products and functionalized magnetic nanoparticles. The amplification and detection procedure take less than 2 h. In this study we also investigated the factors behind the aggregation and confirmed that the size of the padlock probe is a relevant parameter for the amplification efficiency. We compared a 92 and a 69 nt long padlock probe and found the latter to perform over 4 times better than the 92 nt padlock probe. This effect was related to a higher quantity of amplification products produced by the shorter padlock probe. Consequently, the quantity of amplified DNA products affects the aggregation in a positive way, and thanks to it, a better assay sensitivity was achieved. Finally, using our developed method, we could detect as little as 1 amol of the antibiotic-resistance gene *sul1* from a sample containing a multiresistance plasmid. We were also able to quantify the amount of plasmid DNA through absorbance spectroscopy and AC susceptometry. The presented results form the foundation of future development of an ultrasensitive and cheap detection approach that could be used in point of care settings.

1. Introduction

Antibiotic resistance is a rising problem worldwide, and considered by the World Health Organization "one of the biggest threats to global health" (World Health Organization, 2020). Identification of the causative pathogen as well as determination of potential resistance to antibiotics is crucial. However, current testing for the presence of antimicrobial resistant bacteria can take over 48 h and this is insufficient for accurate and timely treatment. Point of care (POC) testing can reduce the time to complete diagnosis and help guide proper antibiotic treatment improving treatment outcome for the patient (Burnham et al., 2017). This will also reduce unnecessary use of antibiotics and thereby slow down development of antibiotic resistance, as currently antibiotics are often over-prescribed (Antoñanzas et al., 2021; Pouwels et al., 2018).

Methods of detecting nucleic acids are of interest in POC settings as they can provide important information about the kind of pathogen causing an infection or detect specific genes conferring resistance to drugs (Niemz et al., 2011; Subsoontorn et al., 2020; Zheng et al., 2021). But for most methods, detection of DNA or RNA is usually preceded by either growth of the bacterium or direct amplification of the nucleic acid, as the quantities found in patient samples are often too small to readily detect. The most common way of amplifying DNA is by polymerase chain reaction (PCR). While PCR is very efficient, it is not always available on short notice for patients in small clinics or third world countries. Other amplification methods, such as isothermal amplification techniques, are better suited for POC (Oliveira et al., 2021) as they can be performed easily, with less and cheaper materials and instrumentation. These techniques can amplify nucleic acids at a constant temperature, eliminating the need for thermocycler instruments, and tend to be simpler, requiring less well-trained personnel. Some examples are rolling circle amplification (RCA), circle-to-circle amplification (C2CA) and loop-mediated isothermal amplification (LAMP) (Dahl et al., 2004; Oliveira et al., 2021).

RCA and C2CA generally use a linear probe binding to a specific target at the 3′ and 5′ ends and circularize. These so-called padlock

* Corresponding author.
E-mail address: teresa.zardan@angstrom.uu.se (T. Zardán Gómez de la Torre).

https://doi.org/10.1016/j.biosx.2022.100277
Received 29 September 2022; Received in revised form 25 October 2022; Accepted 28 October 2022
Available online 4 November 2022

probes (PLPs) are synthetic and have a 5' phosphate to allow ligation upon binding. The ligation is specific enough to be inhibited by the presence of single nucleotide polymorphisms (Edwards et al., 2009; Nilsson et al., 1994). Once the probes are circularized, they allow continuous polymerization of the circular template, creating long ssDNA products (Banér et al., 1998). In C2CA, after the first amplification, the RCA products are digested to monomers. The monomers are ligated and amplified by another RCA, with a much higher starting target DNA quantity, to generate a new set of rolling circle amplification products (RCPs) (Dahl et al., 2004).

Several techniques have been developed to detect RCPs, such as fluorescence-based methods (Kühnemund et al., 2014), colorimetry (Hamidi and Perreault, 2019), electrophoresis (Boss and Arenz, 2020) and electrochemical readouts (Shen et al., 2019). Magnetic particle-based detection is another alternative. Since the last decade, there has been an increase in interest in using magnetic nanoparticles (MNPs) for development of magnetic biosensors. This is because MNPs are very stable and not sensitive to light (Varadan et al., 2008). Magnetic biosensors offer an attractive and cost-effective way for detection of DNA, since the MNPs and the read-out component are relatively inexpensive to produce.

We have recently demonstrated an RCA-based detection method that generates visible aggregates of RCPs and MNPs functionalized with complementary detection oligonucleotides (DO) (Sánchez Martín et al., 2021b). The method provided a limit of detection (LOD) of 0.4 fmol of synthetic target.

To improve the sensitivity of the assay we have integrated and optimized the detection approach with the C2CA technique. In doing so, we have also studied parameters of the used PLPs and the amplification products to improve aggregation, sensitivity and speed. Finally, we apply our detection method for the first time with biological samples where we focus on detecting an antibiotic resistance gene, *sul1*, that confers resistance to sulfonamides, from a multiresistance plasmid. These antibiotics were the first wide-spectrum antibiotics used, and they work by preventing the bacterial synthesis of folic acid, and thus of nucleic acids (Connor, 1998), and are still an important class of antibiotics.

2. Materials and methods

2.1. Magnetic nanoparticles

Commercially available core-shell MNPs were used for this study. They contained a core of 75–80% wt% magnetite, encapsulated in crosslinked hydroxyethyl starch, and coated with streptavidin. The nominal size of the particles was 100 nm diameter and were suspended in PBS at a concentration of 10 mg/ml. They were purchased from Micromod Partikeltechnologie, Germany (product code 10-19-102). The product specifications can be found at their website, along with characterization analysis of the nanoparticles. The theory behind the dynamic magnetic properties of the nanoparticles can be found in Sánchez Martínet al.2021 (Sánchez Martín et al., 2021b).

2.2. Other reagents used in this study

Oligonucleotides were purchased from Biomers, Ulm, Germany. Oligonucleotides used in this study are listed in Table 1. Tth Ligase was purchased from GeneCraft, Köln, Germany. Any other reagents were purchased from Thermo Fisher Scientific, Waltham, MA, USA, unless otherwise specified.

2.3. Particle surface functionalization

The streptavidin coated MNPs were washed thrice with washing buffer (6.6 mM Tris-HCL pH 8, 3.3 mM EDTA, 66 mM NaCl, 0.06% Tween-20) using a permanent magnet. After the washing, the particles were then resuspended in washing buffer to a final MNP concentration of 4 mg/ml and biotin-tagged DO were thereafter added to a final concentration of 240 mM.

2.4. C2CA using synthetic target

Ligation of the padlock probes (PLPs) was carried out in a mixture of DNA target at the desired concentrations, 100 nM PLP, 0.2 mg/ml BSA, 1x Tth Ligase buffer and 250 mU/μL Tth Ligase at 60 °C for 5 min.

Streptavidin-coated My One T1 Dynabeads (also refer as Dynabeads) were washed thrice in washing buffer using a permanent magnet and resuspended in the same buffer at a concentration of 10 mg/ml 50 μg of the washed Dynabeads were added to the ligation mix to bind the target-PLP circles for amplification. The target-PLP circles were captured on the Dynabeads via the 5' biotin on the target by letting the samples incubate at room temperature for 5 min, allowing proper binding.

To isolate the PLP-target-Dynabead complexes from other molecules in the sample the Dynabeads coupled to the target DNA were washed once with 40 μL washing buffer using a permanent magnet. The washing buffer was removed and the circles formed in the ligation reaction were amplified by addition of 20 μL of 0.2 mg/ml BSA, 1x phi29 buffer, 125 μM dNTPs and 100 mU/μL phi29 polymerase, and the reaction was incubated for 20 min (unless otherwise specified) at 37 °C, and inactivated for 2 min at 70 °C.

To digest the RCA products and create a new set of circles, 5 μL of a digestion mix containing 600 nM restriction oligo, 0.2 mg/ml BSA, 1x phi29 buffer and 600 mU/μL *Alu*I restriction enzyme was added to the RCA products. The reaction was carried out for 3 min at 37 °C and *Alu*I was inactivated for 2 min at 70 °C.

The digestion products were isolated from the Dynabeads in solution using a permanent magnet, which pulled the beads out of the solution. Then, 20 μL of a new mix were added, containing 0.2 mg/ml BSA, 1x phi29 buffer, 1.35 mM ATP, 125 μM dNTPs, 150 mU/μL T4 Ligase and 150 mU/μL phi29 polymerase. The reactions ran for 60 min (unless

Table 1
Oligonucleotides used in this work.

Name	Sequence
92 nt Padlock Probe C2CA[a]	5′- taggttgagcccagggacttctagagtgtaccgacctcagtagctgtgactatcgac ttgttgatgtcatgtgtcgcaccaaatgcgattcc -3′
69 nt Padlock Probe C2CA[a]	5′- taggttgagcccagggacctcagtagctgtgactatgttgatgtcatgtgtcgcaccaa atgcgattcc -3′
Restriction Oligo 1RCA	5′- acctcagtagctgtgactat -3′
Restriction Oligo C2CA	5′- atagtcacagctactgaggt -3′
69 nt Padlock Probe C2CA *sul1*[b]	5′- cgtattgcgccgctacctcagtagctgtgactatctggcattctggtgatagcct ccgatgagatcaga -3′
Capture Oligo *sul1*[b]	Biotin-5′- ttttttttttttttttttttgtccgatcagatgcaccgtgtttcaatcgac -3′
Synthetic Target C2CA	Biotin-5′- ccctgggctcaacctaggaatcgcatttg -3′
Detection Oligonucleotide C2CA[a]	Biotin-5′- ttttttttttttttttttttgtgcgacacatgacatcaac -3′
Detection Oligonucleotide 1RCA 5'[a]	Biotin-5' – ttttttttttttttttttttgttgatgtcatgtgtcgcac 3′
Detection Oligonucleotide 1RCA 3'[a]	5′ taggttgagcccagggttttttttttttttttttt – 3′-Biotin-TEG
Detection Oligonucleotide C2CA *sul1*[b]	Biotin-5′- ttttttttttttttttttttggctatcaccagaatgcct -3′

[a] For optimization work, targeting the synthetic target C2CA or the RCA products.
[b] Oligos targeting the biological target, *sul1*.

otherwise specified) at 37 °C.

Immediately after the amplification, 5 μL of a 5 M NaCl solution were added to each sample to bring the NaCl concentration to 500 mM. The samples were then incubated at 70 °C for 5 min for inactivation of the phi29 polymerase and T4 ligase and to prepare for the formation of the aggregates. After the incubation, 5 μL of the functionalized MNPs were added to each sample, vortexed, and incubated for 2 min at 70 °C. The samples were thereafter placed at RT to let the C2CA products and MNPs form aggregates.

2.5. RCA using synthetic target

Amplification, dilution and detection of RCA products was performed according to Sánchez Martín et al. 2021 (Sánchez Martín et al., 2021b). Briefly, the procedure for making a RCP stock solution was performed using 4 nM ligated DNA circles consisting of synthetic target C2CA and 92 nt PLP C2CA (see Table 1). The ligation was performed for 15 min at 37 °C and the RCA for 60 min at 37 °C. The RCPs from the stock solution were diluted with 500 mM NaCl solution and split between different tubes, all containing 4 fmol of RCPs.

2.6. Extraction, digestion and amplification using biological target

The biological sample used in this study was plasmid pUUH239.2 (GenBank accession number CP002474.1), originally isolated from *Klebsiella pneumoniae* at Uppsala University hospital. The plasmid DNA was prepared using the Macherey-Nagel, NucleoBond® Xtra Midi kit according to the manufacturer's instructions. This plasmid contains several resistance genes, and in this study the sulfonamide resistance gene 1 (*sul1*) was targeted. A digestion with restriction enzymes *Alu*I and *Bsu*RI would yield a 73 bp fragment of the *sul1* gene easy to detect (bp 191485 to 191557 in the plasmid). A PLP and capture oligo (CO) were designed for it (sequence in Table 1).

For digestion, a solution with 286 ng of plasmid (2 fmol), 1x Tango buffer, 150 mU/μL *Alu*I and 350 mU/μL *Bsu*RI was incubated for 1 h at 37 °C, and the enzymes were thereafter inactivated for 5 min at 65 °C.

The ligation procedure for the samples using the biological target was similar to the ligation procedure using the synthetic target. In this case, the biological target was mixed with 100 nM PLP and 100 nM biotinylated CO before the ligation, and thereafter denatured for 5 min at 95 °C. Afterwards, 0.2 mg/ml BSA, 1x Tth Ligase buffer and 250 mU/μL Tth Ligase were added to the tripartite complex (target sequence, PLP and CO) and the ligation reaction was carried out at 55 °C for 5 min. After the ligation procedure, the circles were captured on 50 μg streptavidin-coated Dynabead particles via the biotinylated CO by letting the samples incubate at room temperature for 5 min.

The amplification and the aggregation procedures were then conducted in the same way as for the samples containing the synthetic target.

2.7. AC susceptibility measurements

The samples were placed in glass vials and PBS was added to bring the volume to 200 μL. Frequency-dependent magnetic susceptibility measurements ($\chi = \chi' + \chi''$) were performed at room temperature, from 5 to 250,000 Hz at 21 logarithmically equidistant frequency points. The measurements were performed in an AC susceptometer (DynoMag, RISE Acreo, Göteborg, Sweden). The frequency-dependent imaginary part of the complex susceptibility, χ'', exhibits a relaxation peak at around 100 Hz for the MNPs used in this work (see Supplementary Fig. 3). The height of the peak, χ''_{max}, is proportional to the number of unbound MNPs in a sample. This value decreases with increasing DNA concentration as the MNPs binds to the RCPs (Sánchez Martín et al., 2021b).

2.8. Absorbance measurements

The samples were placed in a 96-well plate and each sample volume was brought to 200 μL with PBS. Blanks with only 200 μL PBS were measured as well. Absorbance measurements were done at 350 nm, with 10 ms settle time and multiple reads per well (4 × 4 in a circle) at 1500 μm from the well edge. An Infinite® 200 plate reader (Tecan, Sweden) was used for the measurements. Blank values were subtracted from all samples.

2.9. Imaging of samples

Images of the individual aggregates were captured in 96-well plates with an Olympus BX60 optical microscope, using a 4x objective, and an OMAX A3580U3 camera.

Images of the 96-well plates and PCR tubes with aggregates inside were taken with a phone camera.

The samples in Fig. 1 were photographed with a Fujufilm X-T3 camera and a Fujinon XF 90/2 R LM WR lens.

2.10. Limit of detection (LOD) calculation

The LOD was calculated taking the average of three NC samples and subtracting three times the standard deviation from it. Any samples which average plus standard deviation was under the LOD is considered to be detectable.

3. Results and discussion

3.1. Assay process and optimization

In this study we detailed the use of C2CA combined with our previously published work on aggregation of MNPs with RCPs. C2CA adds a second amplification step which gives higher sensitivity since the number of RCPs, or C2CA products, increases. We have further integrated the aggregation and the amplification processes, specifically in the last inactivation step of the enzymes, to make the assay easier and more time efficient. The aggregation step adds as little as 5 extra minutes to the original C2CA protocol (Sánchez Martín et al., 2021a) and the assay time is still less than 2 h. The workflow of the protocol is detailed in Scheme 1. The MNP solutions used in this study have a dark brown color and the hue of the solution becomes lighter when aggregation occur. This allows for naked eye detection, absorbance/turbidity analysis of the solution color and AC susceptibility readout. The AC susceptometer measures the frequency-dependent imaginary part of the complex susceptibility, χ'' where a relaxation peak can be observed at around 100 Hz (see Supplementary Fig. 3). The height of this peak, χ''_{max}, is proportional to the number of unbound MNPs in a sample. This value decreases with increasing DNA concentration as the MNPs binds to the RCPs.

When we initially started to performed C2CA in combination with MNP aggregation, the size of the aggregates was smaller than expected, absorbance and AC susceptometry measurements were worse, and aggregate size inconsistent across samples with equal starting DNA. We decided to perform optimization work in the aggregation step to determine the ideal temperature for aggregation. To do this, three different conditions were evaluated (80 °C and 70 °C for 5 min prior addition of MNPs and 70 °C for 5 min prior addition of MNPs with an extra 2 min after addition of MNPs.) The results of the aggregation are shown in Supplementary Fig. 1. We found that allowing the sample to remain heated after the addition of MNPs generated more reliable results, while cooling the samples immediately after addition of MNPs could lead to improper aggregation (as seen for the 70 °C samples).

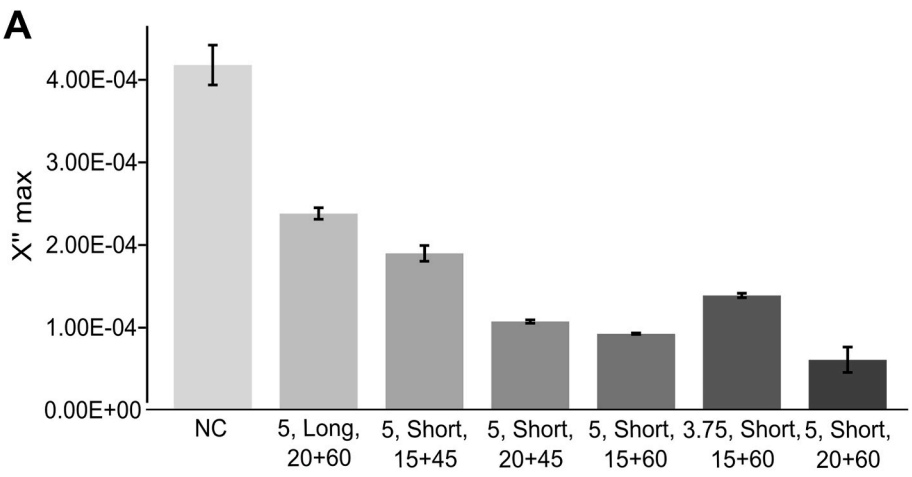

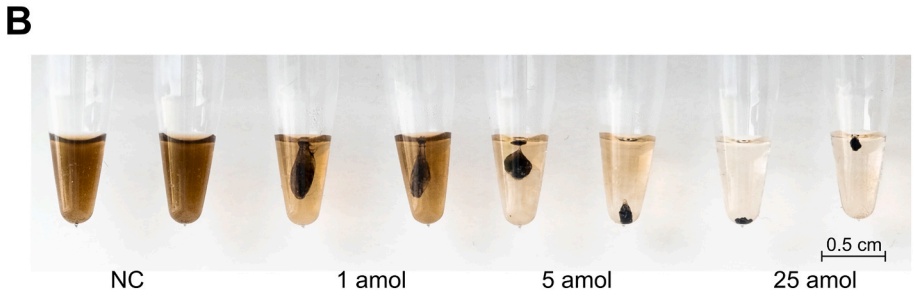

Fig. 1. Assaying the parameters behind aggregation. Average AC susceptometry results (**A**) of duplicates of all tested sample types. The first number on the sample legend determines the quantity of target in amol. Short denotes the use of the 69 nt PLP and Long the use of the 92 nt PLP. The last numbers describe the time in minutes for the first and second amplification steps. Thus, the sample "5, Long, 20 + 60" had 5 amoles of starting target, the 92 nt PLP was used and the first amplification step ran for 20 min and the second for 60 min. Image (**B**) showing aggregates of different sizes formed by different target quantities, using the Short PLP and normal C2CA protocol of 20 + 60 min.

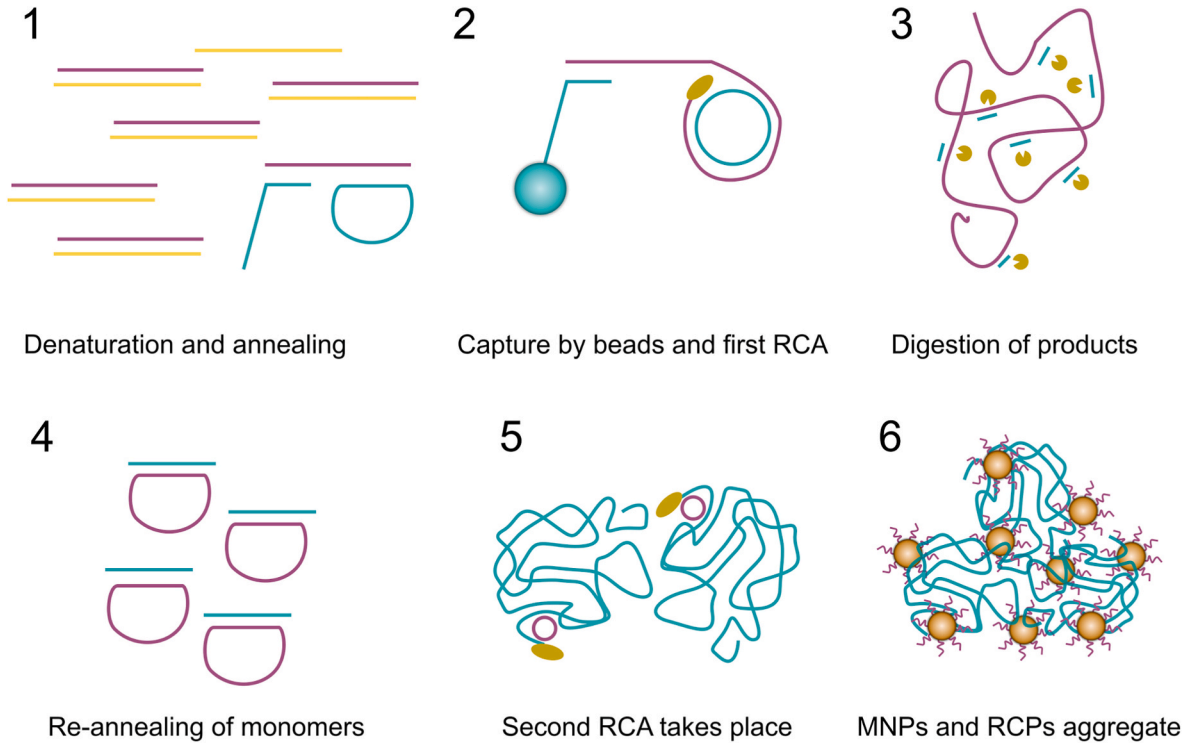

Scheme 1. Schematic illustration of C2CA and detection method. **1.** Digested samples (purple and yellow) are denatured and thereafter hybridize to the PLP (blue circle) and CO (blue line). A ligase enables correctly matched PLP to be circularized **2.** Dynabeads (blue sphere) capture the COs by a streptavidin-biotin interaction and the first RCA follows. **3.** Digestion of the first RCA products is performed with *Alu*I (yellow symbol). **4.** In the same step, reannealing occurs between restriction oligos (blue lines) and the monomers (purple circles), creating new primed circles. **5.** A secondary round of RCA is performed. **6.** Functionalized MNPs (brown spheres) are added and the C2CA products and the MNPs form visible aggregates.

3.2. Forces behind the aggregation process

In our previous study (Sánchez Martín et al., 2021b) we showed that the MNPs interact with the DNA through the binding between the DOs, and the repeated sequences in the amplification products, but we did not perform an in-depth study of different factors driving the aggregation process other than DNA quantity, temperature and salt. Here we investigated different parameters to see what factors positively drive the aggregation. First of all, we hypothesized that a shorter PLP would improve amplification yield and quantity of binding sites. Amplification products of a certain length produced from shorter PLPs will have more repeats, and thus more binding sites for the DOs. Consequentially, a larger quantity of repeats after the first amplification step in C2CA will generate a higher quantity of C2CA products in the second amplification step, as each repeat after the first RCA is used as a PLP for the second RCA. For this study we used a 92 nucleotides (nt) PLP and a 69 nt PLP, both binding to a synthetic *V. cholerae* target, with the same required sequences for both RCA and C2CA. The 69 nt PLP is 75% of the size of the 92 nt PLP, meaning that we expect the same quantity of repeats as in the case of the 92 nt PLP if the amplification time is reduced by 25%. When comparing the products from both PLPs we specifically focused on the quantity of C2CA products, the length of the products, and the quantity of binding sites for the DOs. In C2CA, we can control the quantity of RCPs by changing the incubation time of the first amplification step, the length of the products by the incubation time of the second amplification step, and the quantity of binding sites by a combination of both. For this reason, we changed the amplification times for the two amplification steps and analyzed the samples in the AC susceptometer. Results are shown in Fig. 1A, and full magnetization spectra can be found in Supplementary Fig. 3.

We intended to determine the effect of amplification product length on aggregation. We analyzed and compared the following samples: 5 amol, long PLP, 20 + 60 and 5 amol, short PLP, 15 + 45. The two samples should, in theory, have the same quantity of binding sites, as the amplification times of the shorter PLP have been reduced by 25%. However, for that same reason, the products of the shorter PLP should be 25% shorter in length. We expected length to have a positive impact in aggregation, but in this case the shorter products bind to a larger number of MNPs. This was surprising but the difference could arise from another parameter, such as the amplification efficiency of the PLP. Joffroy et al. (2018) have observed that the length of the PLP affects the polymerization rate and amplification efficiency. This is due to the strain put onto the PLP during polymerization, which changes depending on the turns of the PLP DNA. According to their work, the shorter PLP used here should allow a higher polymerization speed compared to the longer one.

To observe if there was a difference in product quantity produced by the two different PLPs, monomerized C2CA products were observed on a gel. The results are presented in Supplementary Fig. 2 and suggest that there is much more product when amplifying with the 69 nt PLP compared to the 92 PLP. Since the products are longer, it is hard to determine whether the impact comes from the length or having more repeats. But the increase in product quantity seems to be the main driving force behind MNP aggregation.

Finally, to observe the size of aggregates with different quantity of target, we performed a standard C2CA (20 min for the first amplification, and 60 for the second) using the short PLP and synthetic target for *V. cholerae* and photographed the resulting aggregates from samples containing 0 (NC), 1, 5 and 25 amol of target. The photograph is provided in Fig. 1B and shows that aggregates are easily visible in all samples, even when using only 1 amol of target.

We also wanted to investigate how the number of binding sites per amplification product affected aggregation. We assume that more binding sites lead to more MNPs binding, which will in turn promote the aggregation, but the effects of this were hard to determine from previous experiments. Thus, we decided to use a second DO to bind to the repeats of the amplification products at a different site. We hypothesized that increasing the number of binding sites should affect the aggregation positively. Having MNPs that can bind to two regions per repeat instead of one will duplicate the number of binding sites, and would consequently improve the aggregation. To test this, we functionalized the different MNP batches with either one of the DOs (3′ or 5′) or both DOs (3'+5′). We also made a mixture of MNPs functionalized with either the 3′ or 5′ DO (sample 3'/5'). For this experiment, a single RCA was performed (as previously described by Sánchez Martín et al. (Sánchez Martín et al., 2021b)) instead of C2CA. Results are shown in Fig. 2. Interestingly, in this case, having two DO binding sites per PLP repeat does not seem to improve aggregation, all samples have similar absorbance values regardless of whether MNPs are functionalized with either of the DO, both, or a mix of the two DOs. Thus, we moved forward with using only one type of DO.

3.3. Detecting antibiotic resistance gene sul1 in a multi-resistance plasmid

As our next objective, we wanted to investigate the performance of the assay with a biological sample, using the optimized conditions. For that, we acquired the multi-resistance plasmid pUUH239.2, which was isolated from a *Klebsiella pneumoniae* clone causing an outbreak at the Uppsala University Hospital. This plasmid contains a large resistance cassette with genes conferring resistance to a wide variety of antibiotics (Sandegren et al., 2012). We decided to target *sul1*, a gene that gives bacteria resistance to sulfonamides.

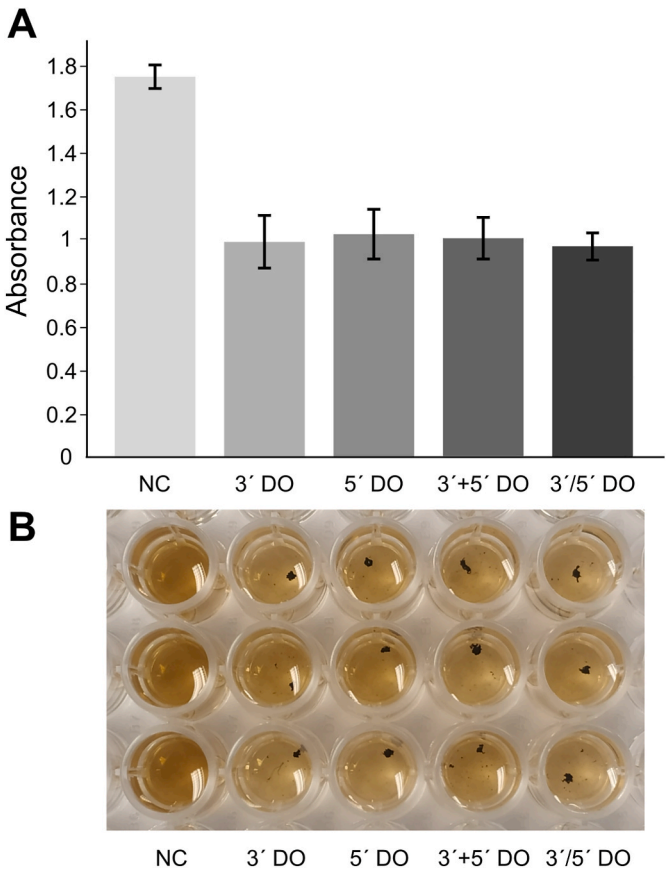

Fig. 2. Analyzing how the number of binding sites affects aggregation. Absorbance readouts (**A**) of NC and positive samples with 4 fmol of *V. cholerae* target amplified by a single RCA. Error bars represent SD of N = 3. Image of the plate (**B**) with samples before measurement. 3′ and 5′represent the end the biotin is at, discriminating between the two oligos used. Both sequences can be found in Table 1. MNPs used in samples 3′+5′ were functionalized with a mix of both oligos, in same proportions. MNPs used in samples 3′/5′ were an equal mix of MNPs functionalized only with one or the other, in equal proportions.

The results of using the optimized C2CA method with the digested plasmid are shown in Fig. 3. AC susceptometry (Fig. 3A) and absorbance (Fig. 3B) results prove that 1 amole of target is distinguishable from the NCs. From the image taken on the 96-well plate (Fig. 3C) we can see the aggregates present for all positive samples. The samples imaged in Fig. 3C are the same that were measured for the absorbance results. The full magnetization spectra of all samples can be found in Supplementary Fig. 4. Samples at 1 amole contain aggregates that have broken slightly, this is due to the pipetting of buffer onto the samples. Nevertheless, we show that visual identifications of samples as low as 1 amole is possible with our developed method.

While in this study we have used samples containing isolated plasmids from *Klebsiella pneumoniae*, the same procedure can also be performed with clinical samples. The Dynabeads, used after the ligation step, have the ability to capture the DNA targets of interest and separate it from rest of the sample. This could also easily be implemented in clinical samples. In addition, the assay can easily be modified and extended to new targets by designing new complementary PLPs and DOs. Furthermore, RCA has already been proven to work on patient samples (Ciftci et al., 2020; Mezger et al., 2014).

Other methods have been used to detect DNA of infectious disease-causing agents, with varying results: In Table 2, we have compared our developed method with other detection methods based on isothermal amplification. As expected, C2CA provides better sensitivity than RCA in a similar amount of time, due to the two rounds of amplification. Our method has advantages over other aggregation-based detection methods. Other RCA-based approaches using aggregation have a high sensitivity but take much longer time (Ding et al., 2013). LAMP-based assays still manage faster amplification, but are more prone to false positives (Chou et al., 2011), and in several of the studies listed in the table, the aggregation between DNA and nanoparticles is unspecific (Lin et al., 2013; Suwannin et al., 2021), unlike in our method, where a specific oligo recognizes the amplified sequence. Overall, the success of integrating sequence-specific MNP aggregation

Table 2
Comparison of different detection methods based on isothermal amplification and particle aggregation.

Amplification method	Read-out method	LOD	Assay time	Reference
LAMP	Colorimetric (Au aggregation)	–	90 min	Veigas et al. (2013)
LAMP	Colorimetric (Au aggregation)	1 parasite/ul	Less than 1 h	Suwannin et al. (2021)
RCA	Electrochemical (Au aggregation)	3 amol	6 h	Ding et al. (2013)
RCA	Colorimetric (Au aggregation)	70 fM	Less than 4 h	Li et al. (2010)
RCA	Visual (MNP aggregation)	0.62 amol	6 h	Lin et al. (2013)
RCA	Visual (MNP aggregation)	0.4 fmol	Less than 2 h	Sánchez Martín et al. (2021b)
C2CA	Visual, spectroscopy and magnetic	1 amol	Less than 2 h	Current work
C2CA	Electrophoretic detection in microchip	25 ng bacterial gDNA	65 min	Mahmoudian et al. (2008)
C2CA	Fluorescence microscopy	1 aM	Over 1 h	Kühnemund et al. (2014)
C2CA	Optomagnetic	0.4 fM	100 min	Tian et al. (2020)

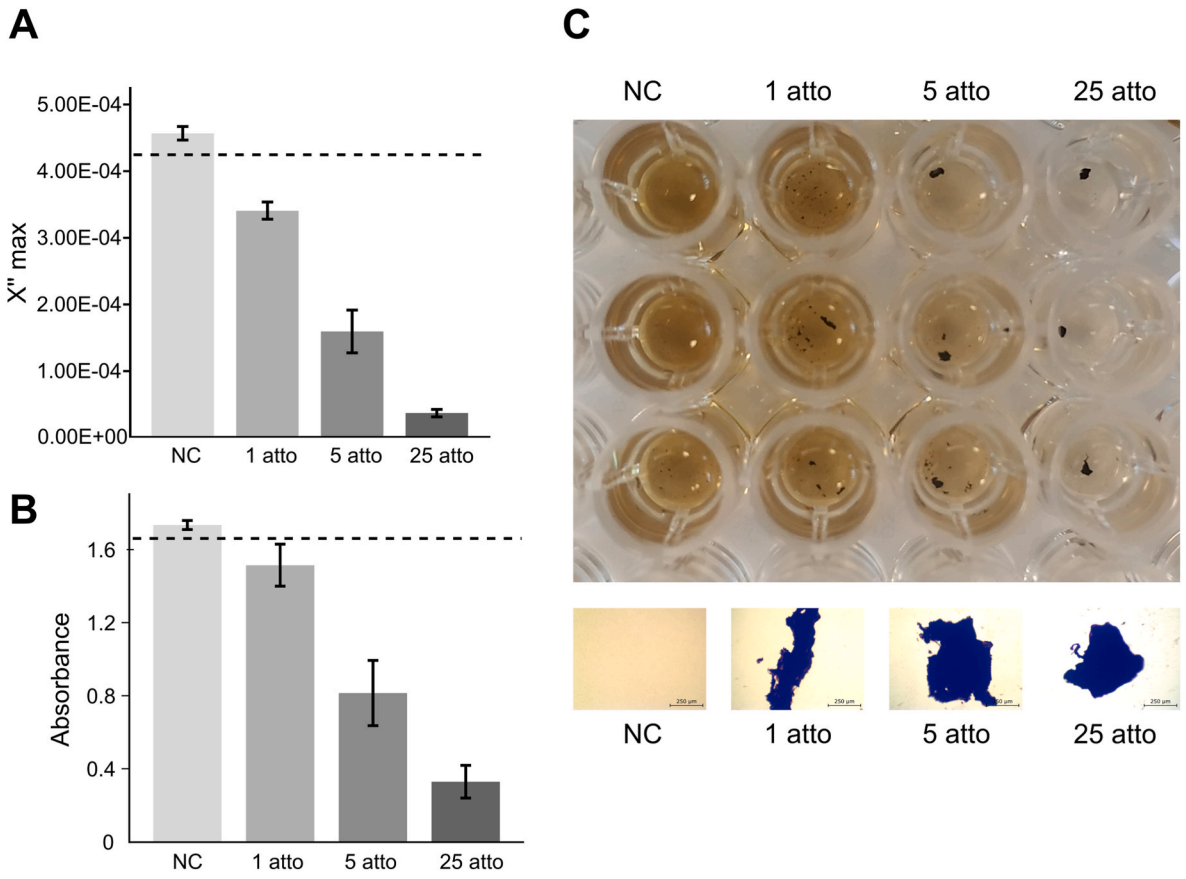

Fig. 3. Detection of resistance gene *sul1*. Detection can be done using an AC susceptometer (**A**), an absorbance reader (**B**) or visually (**C**). Both methods are able to detect 1 amole of starting target DNA. Error bars represent standard deviation of N = 3. Dashed lines represent LOD.

with the C2CA method in a seamless way, adding only 5 min of time, is the main benefit of our new approach. While other C2CA-based studies that do not use aggregation for detection show similar or higher sensitivity, all of them require more complicated methods of detecting the presence of the amplified DNA, such as fluorescence microscopy (Kühnemund et al., 2014), electrophoresis (Mahmoudian et al., 2008) or optomagnetic sensors (Tian et al., 2020). These do not allow for quick results in multiple samples at the same time, and the time required by these techniques can vary, but in every case, it is more than the time required to visually inspect samples for the presence of aggregates. On top of that they require more equipment, some of which might not be easy to use, limiting even further their use for POC.

3.4. Selectivity of the padlock probes and Dynabeads

Finally, we wanted to make sure that if the target for a PLP was not present in a biological sample, we would not have false positive results. The plasmid we used contained over 220 kb, so there is a chance that on such high concentration some sequence might bind unspecifically to a PLP and ligate it. The PLPs only ligate when bound to matching sequences, and the Dynabeads should not pull unwanted sequences and unreacted PLPs into the first RCA reaction. For this, we added 0, 25 and 100 amol of digested plasmid and performed a normal C2CA, swapping the *sul1* PLP for the PLP used in optimization, which should not bind to the plasmid sequences. MNPs for detection were functionalized with the optimization Detection Oligonucleotide as well to detect any amplification products from the mismatched PLPs. The samples contained no aggregates, and an image of the samples and the full magnetization spectra can be found on Supplementary Fig. 5. On Fig. 4 we can observe the AC susceptometry peaks representing the free nanoparticles, with no significant changes between the negative control and positive samples. This indicates that no detectable amplification of mismatched PLP was found in our samples.

4. Conclusions

The formation of aggregates induced by specific binding between MNPs and C2CA products allows for rapid visual detection of specific DNA sequences. In this work, we have achieved our primary goal of successfully integrate the aggregation step with the C2CA technique, and to further optimized the fully integrated method. By integrating these two methods it is possible to detect at least 1 amol of a specific gene, *sul1*, from a 220 kb plasmid. We showed that qualitative detection is possible through naked-eye detection and quantification of the DNA in the samples is possible using a spectrophotometer and/or an AC susceptometer. While the spectrophotometer is not as sensitive and accurate as the AC susceptometry, it allows to analyze multiple samples at the same time and in a short period of time.

Furthermore, we confirmed that the size of the PLPs impact the yield of RCA and C2CA. A shorter PLP yields a higher quantity of amplification products which in turn yields a better assay sensitivity. However, having two available binding sites in the amplification products and using two different DOs, complementary to the two binding sites, did not improve the aggregation compared to using one type of DO. Lastly, we show that the PLP ligation and the Dynabead target isolation are highly specific, showing no detectable amplification of a mismatched PLP in 100 amol of plasmid in a normal C2CA.

As a next step we intend to further optimize the method to increase its performance. This can, for example, be done by improving the PLPs more, using different particle types and sizes and changing the RCA times. To move closer to the development of a POC diagnostic test, it would be strongly advantageous if our method could be performed in a fully integrated microfluidic chip, which we intend to investigate further. C2CA has been already integrated in microfluidic chips (Kühnemund et al., 2014), and we believe this is also possible with our developed method.

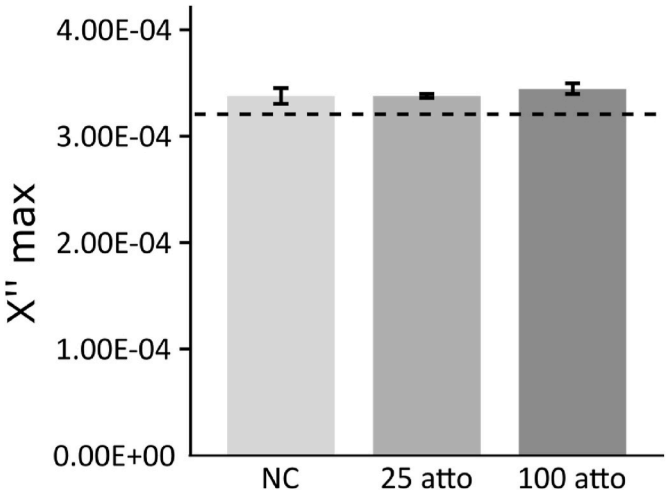

Fig. 4. Selectivity of PLPs and Dynabeads. Mismatched PLPs do not result in detectable amplification products, due to low chance of ligation and Dynabead isolation of target from the bulk of plasmid DNA in solution. Image shows AC susceptometry results of C2CA with mismatched target-PLP sequences. Error bars represent standard deviation of N = 3. Dashed line represents the LOD.

Naked-eye detection is a great asset if we consider that the idea for this technique is to be used in POC settings. The proposed method does not require any expensive read-out instrumentation to interpreted or process results which will make lower the future manufacturing cost. This will in turn allow smaller clinics and other healthcare settings, especially in underdeveloped countries, to have an easier and cheaper way of detecting pathogenic DNA and antibiotic resistance.

CRediT authorship contribution statement

Darío Sánchez Martín: Conceptualization, Methodology, Validation, Investigation, Writing – original draft, Visualization. **Marie Wrande:** Methodology, Validation, Investigation, Writing – review & editing. **Linus Sandegren:** Methodology, Validation, Resources, Writing – review & editing. **Teresa Zardán Gómez de la Torre:** Conceptualization, Methodology, Validation, Resources, Writing – review & editing, Supervision.

Declaration of competing interest

The authors declare that they have no known competing financial interests or personal relationships that could have appeared to influence the work reported in this paper.

Data availability

Data will be made available on request.

Acknowledgements

This work was supported by The Uppsala Antibiotic Center.

Appendix A. Supplementary data

Supplementary data to this article can be found online at https://doi.org/10.1016/j.biosx.2022.100277.

References

Antoñanzas, F., Juárez-Castelló, C.A., Rodríguez-Ibeas, R., 2021. Using point-of-care diagnostic testing for improved antibiotic prescription: an economic model. Health Econ. Rev. 11, 1–12. https://doi.org/10.1186/s13561-021-00326-y.

Banér, J., Nilsson, M., Mendel-Hartvig, M., Landegren, U., 1998. Signal amplification of padlock probes by rolling circle replication. Nucleic Acids Res. 26, 5073–5078. https://doi.org/10.1093/nar/26.22.5073.

Boss, M., Arenz, C., 2020. A fast and easy method for specific detection of circular RNA by rolling-circle amplification. Chembiochem 21, 793–796. https://doi.org/10.1002/cbic.201900514.

Burnham, C.A.D., Leeds, J., Nordmann, P., O'Grady, J., Patel, J., 2017. Diagnosing antimicrobial resistance. Nat. Rev. Microbiol. 15, 697–703. https://doi.org/10.1038/nrmicro.2017.103.

Chou, P.H., Lin, Y.C., Teng, P.H., Chen, C.L., Lee, P.Y., 2011. Real-time target-specific detection of loop-mediated isothermal amplification for white spot syndrome virus using fluorescence energy transfer-based probes. J. Virol. Methods 173, 67–74. https://doi.org/10.1016/j.jviromet.2011.01.009.

Ciftci, S., Neumann, F., Abdurahman, S., So, K., Mirazimi, A., Nilsson, M., 2020. Digital Rolling Circle Ampli fi cation e Based Detection of Ebola and Other Tropical Viruses 22. https://doi.org/10.1016/j.jmoldx.2019.10.014.

Connor, E.E., 1998. Sulfonamide antibiotics. Prim. Care Update Ob. Gyns. 5, 32–35. https://doi.org/10.1016/S1068-607X(97)00121-2.

Dahl, F., Banér, J., Gullberg, M., Mendel-Hartvig, M., Landegren, U., Nilsson, M., 2004. Circle-to-circle amplification for precise and sensitive DNA analysis. Proc. Natl. Acad. Sci. U.S.A. 101, 4548–4553. https://doi.org/10.1073/pnas.0400834101.

Ding, C., Wang, N., Zhang, J., Wang, Z., 2013. Rolling circle amplification combined with nanoparticle aggregates for highly sensitive identification of DNA and cancer cells. Biosens. Bioelectron. 42, 486–491. https://doi.org/10.1016/j.bios.2012.10.015.

Edwards, K.J., Reid, A.L., Coghill, J.A., Berry, S.T., Barker, G.L.A., 2009. Multiplex single nucleotide polymorphism (SNP)-based genotyping in allohexaploid wheat using padlock probes. Plant Biotechnol. J. 7, 375–390. https://doi.org/10.1111/j.1467-7652.2009.00413.x.

Hamidi, S.V., Perreault, J., 2019. Simple rolling circle amplification colorimetric assay based on pH for target DNA detection. Talanta 201, 419–425. https://doi.org/10.1016/j.talanta.2019.04.003.

Joffroy, B., Uca, Y.O., Prešern, D., Doye, J.P.K., Schmidt, T.L., 2018. Rolling circle amplification shows a sinusoidal template length-dependent amplification bias. Nucleic Acids Res. 46, 538–545. https://doi.org/10.1093/nar/gkx1238.

Kühnemund, M., Witters, D., Nilsson, M., Lammertyn, J., 2014. Circle-to-circle amplification on a digital microfluidic chip for amplified single molecule detection. Lab Chip 14, 2983–2992. https://doi.org/10.1039/c4lc00348a.

Li, J., Deng, T., Chu, X., Yang, R., Jiang, J., Shen, G., Yu, R., 2010. Rolling circle amplification combined with gold nanoparticle aggregates for highly sensitive identification of single-nucleotide polymorphisms. Anal. Chem. 82, 2811–2816. https://doi.org/10.1021/ac100336n.

Lin, C., Zhang, Y., Zhou, X., Yao, B., Fang, Q., 2013. Naked-eye detection of nucleic acids through rolling circle amplification and magnetic particle mediated aggregation. Biosens. Bioelectron. 47, 515–519. https://doi.org/10.1016/j.bios.2013.03.056.

Mahmoudian, L., Kaji, N., Tokeshi, M., Nilsson, M., Baba, Y., 2008. Rolling circle amplification and circle-to-circle amplification of a specific Gene Integrated with Electrophoretic Analysis on a Single Chip, 80, pp. 2483–2490.

Mezger, A., Christina, O., Herthnek, D., Blomberg, J., Nilsson, M., 2014. Detection of rotavirus using padlock probes and rolling circle amplification. PLoS One 9. https://doi.org/10.1371/journal.pone.0111874.

Niemz, A., Ferguson, T.M., Boyle, D.S., 2011. Point-of-care nucleic acid testing for infectious diseases. Trends Biotechnol. 29, 240–250. https://doi.org/10.1016/j.tibtech.2011.01.007.Point-of-care.

Nilsson, M., Malmgren, H., Samiotaki, M., Kwiatkowski, M., Chowdhary, B.P., Landegren, U., 1994. Padlock probes: circularizing oligonucleotides for localized DNA detection. Science (80- 265, 2085–2088. https://doi.org/10.1126/science.7522346.

Oliveira, B.B., Veigas, B., Baptista, P.V., 2021. Isothermal amplification of nucleic acids: the race for the next "gold standard. Front. Sensors 2, 1–22. https://doi.org/10.3389/fsens.2021.752600.

Pouwels, K.B., Dolk, F.C.K., Smith, D.R.M., Robotham, J.V., Smieszek, T., 2018. Actual versus "ideal" antibiotic prescribing for common conditions in English primary care. J. Antimicrob. Chemother. 73 https://doi.org/10.1093/jac/dkx502 ii19–ii26.

Sánchez Martín, D., Oropesa-Nuñez, R., Zardán Gómez de la Torre, T., 2021a. Evaluating the performance of a magnetic nanoparticle-based detection method using circle-to-circle amplification. Biosensors 11, 173.

Sánchez Martín, D., Oropesa-Nuñez, R., Zardán Gómez De La Torre, T., 2021b. formation of visible aggregates between rolling circle amplification products and magnetic nanoparticles as a strategy for point-of-care diagnostics. ACS Omega 6, 32970–32976. https://doi.org/10.1021/acsomega.1c05047.

Sandegren, L., Linkevicius, M., Lytsy, B., Melhus, Å., Andersson, D.I., 2012. Transfer of an Escherichia coli ST131 multiresistance cassette has created a Klebsiella pneumoniae-specific plasmid associated with a major nosocomial outbreak. J. Antimicrob. Chemother. 67, 74–83. https://doi.org/10.1093/jac/dkr405.

Shen, C., Liu, S., Li, X., Yang, M., 2019. Electrochemical detection of circulating tumor cells based on DNA generated electrochemical current and rolling circle amplification. Anal. Chem. 91, 11614–11619. https://doi.org/10.1021/acs.analchem.9b01897.

Subsoontorn, P., Lohitnavy, M., Kongkaew, C., 2020. The diagnostic accuracy of isothermal nucleic acid point-of-care tests for human coronaviruses: a systematic review and meta-analysis. Sci. Rep. 10, 1–13. https://doi.org/10.1038/s41598-020-79237-7.

Suwannin, P., Polpanich, D., Leelayoova, S., Mungthin, M., Tangboriboonrat, P., Elaissari, A., Jangpatarapongsa, K., Ruang-areerate, T., Tangchaikeeree, T., 2021. Heat-enhancing aggregation of gold nanoparticles combined with loop-mediated isothermal amplification (HAG-LAMP) for Plasmodium falciparum detection. J. Pharm. Biomed. Anal. 203, 114178 https://doi.org/10.1016/j.jpba.2021.114178.

Tian, B., Gao, F., Fock, J., Dufva, M., Fougt, M., 2020. Biosensors and Bioelectronics Homogeneous circle-to-circle amplification for real-time optomagnetic detection of SARS-CoV-2 RdRp coding sequence. Biosens. Bioelectron. 165, 112356 https://doi.org/10.1016/j.bios.2020.112356.

Varadan, V.K., Chen, L., Xie, J., 2008. Nanomedicine-Design and Applications of Magnetic Nanomaterials, Nanosesnsors and Nanosystems. John Wiley & Sons Ltd., United Kingdom.

Veigas, B., Pedrosa, P., Couto, I., Viveiros, M., Baptista, P.V., 2013. Isothermal DNA amplification coupled to Au-nanoprobes for detection of mutations associated to Rifampicin resistance in Mycobacterium tuberculosis. J. Nanobiotechnol. 11, 1–6. https://doi.org/10.1186/1477-3155-11-38.

World Health Organization, 2020. Antibiotic Resistance [WWW Document]. URL. https://www.who.int/news-room/fact-sheets/detail/a.

Zheng, C., Wang, K., Zheng, W., Cheng, Y., Li, T., Cao, B., Jin, Q., Cui, D., 2021. Rapid developments in lateral flow immunoassay for nucleic acid detection. Analyst 146, 1514–1528. https://doi.org/10.1039/d0an02150d.